

# Fe-doped and (Zn, Fe) co-doped CdS films: Could the Zn doping affect the concentration of $\text{Fe}^{2+}$ and the optical properties?

Kewei Liu<sup>a,b</sup>, J.Y. Zhang<sup>a,\*</sup>, Xiaojie Wu<sup>a,b</sup>, Binghui Li<sup>a</sup>, Bingsheng Li<sup>a</sup>,  
Youming Lu<sup>a</sup>, Xiwu Fan<sup>a</sup>, Dezhen Shen<sup>a</sup>

<sup>a</sup>Key Laboratory of Excited State Processes, Changchun Institute of Optics, Fine Mechanics and Physics, Changchun 130033, China

<sup>b</sup>Graduate School of the Chinese Academy of Sciences, Beijing 100049, China

Received 8 March 2006; received in revised form 16 May 2006; accepted 25 June 2006

## Abstract

$\text{Cd}_{1-x}\text{Fe}_x\text{S}$  and  $\text{Cd}_{1-x-y}\text{Fe}_x\text{Zn}_y\text{S}$  thin films were grown by low-pressure metal organic chemical vapor deposition (LP-MOCVD) on  $c\text{-Al}_2\text{O}_3$  substrates. The films fabricated at  $360^\circ\text{C}$  under an hydrogen pressure of 76 Torr had hexagonal structure with only one (0002) diffraction peak. The samples with low doping content have sharp absorption edges. It is found that the absorption edge and the emission peak positions of the  $\text{Cd}_{1-x-y}\text{Fe}_x\text{Zn}_y\text{S}$  film shift to high energy due to the Zn-doping. The band gap energy could be tuned in a wide range with the change of Zn content. The broadening of the  $\text{Cd}_{1-x-y}\text{Fe}_x\text{Zn}_y\text{S}$  emission peak could be attributed to the alloy fluctuations and the shallow defect in the samples.

© 2006 Elsevier B.V. All rights reserved.

PACS: 71.20.Nr; 71.55.Gs; 78.20.-e; 61.10.Nz

Keywords:  $\text{Cd}_{1-x-y}\text{Fe}_x\text{Zn}_y\text{S}$ ; Absorption edges; Band gap energy

## 1. Introduction

During the last few years, there has been much interest in dilute magnetic semiconductors (DMS). DMSs are II–VI, IV–VI, or III–V compounds in which fraction of non-magnetic cations has been substituted by magnetic transition metal or rare-earth metal ions [1]. Most reports so far on these materials have focused on Mn, Fe, or Co monodoped DMS [2–15], and few co-doped DMS materials have been reported [16]. It is well-known that co-doping can lead to remarkable change of the properties of DMS. Room temperature ferromagnetic can be observed for (Fe, Cu) co-doped ZnO film [17]. The Faraday rotations  $\theta_F$  of CdMnCoTe and CdMnFeTe films were enhanced comparing with that of CdMnTe [18]. The Co-doped ZnO thin films showed a metallic conducting characteristic with low resistance, while the (Mn, Co) co-doped ZnO thin film had semiconductor conductivity with high resistance [19].

However, very limited information is available on the film quality, the optical and electronic properties of the co-doped CdS-based DMS materials.

CdS-based DMS is a good candidate for such applications as magneto-optical devices (magnetic field sensors, isolators and magneto-optical switches), field-emission displays, solar cells and gas sensors. In this letter, we prepared  $\text{Cd}_{1-x}\text{Fe}_x\text{S}$  and  $\text{Cd}_{1-x-y}\text{Fe}_x\text{Zn}_y\text{S}$  films with well preferred orientation on  $c\text{-Al}_2\text{O}_3$  using MOCVD. The structure and composition of the films were characterized by the X-ray diffraction (XRD) and the energy dispersive spectroscopy (EDS). We have also investigated the optical and electrical properties of the films at room temperature.

## 2. Experiment

$\text{Cd}_{1-x}\text{Fe}_x\text{S}$  and  $\text{Cd}_{1-x-y}\text{Fe}_x\text{Zn}_y\text{S}$  thin films were grown by a LP-MOCVD system with a horizontal rectangular quartz reactor. The ironpentacarbonyl ( $\text{Fe}(\text{CO})_5$ ), dimethylcadmium (DMCd), dimethylzinc (DMZn) and

\*Corresponding author. Tel.: +86 431 6176322.

E-mail address: [zhangjy53@yahoo.com.cn](mailto:zhangjy53@yahoo.com.cn) (J.Y. Zhang).

Table 1  
Typical growth conditions for epitaxial films on (0001) Al<sub>2</sub>O<sub>3</sub> substrates

Film	<i>P</i> (Torr)	<i>T<sub>g</sub></i> (°C)	Total H <sub>2</sub> (sccm)	Fe(CO) <sub>5</sub> (0°C) (sccm)	DMCd (−5°C) (sccm)	DEZn (5°C) (sccm)	H <sub>2</sub> S (2 atm) (sccm)
CdFeS	76	360	1900	1,4,7,10	8	0	13
CdZnFeS	76	360	1900	1,4,7,10	8	2	13

hydrogen sulphide (H<sub>2</sub>S) gas were used as source materials for Fe, Cd, Zn and S, respectively. The sapphire with (0001) orientation (*c*-face) was used as the substrate. Before loaded into the reaction chamber, the substrates were cleaned by acetone and ethanol for 5 min in an ultrasonic bath and etched in an acid solution (3H<sub>2</sub>SO<sub>4</sub> + 1H<sub>3</sub>PO<sub>4</sub>) for 5 min at 160°C, followed by a de-ionized water rinse. Then the substrates were heated at 600°C for 10 min in H<sub>2</sub> flow. During deposition, DMCd precursor is kept in a bubbler cooled to −5°C and transported into the reactor flowing at 8 ml/min. H<sub>2</sub>S gas is introduced separately into the reactor and the flow rate is kept at 13 ml/min. Fe(CO)<sub>5</sub> is cooled down to 0°C with the flow rate ranging from 0 to 10 ml/min. DEZn is kept at 5°C with the flow rate of 2 ml/min. All the depositions were operated at the pressure of 76 Torr and the growth temperature (*T<sub>g</sub>*) was kept at 360°C. The typical growth conditions are shown in Table 1.

The structural and composition of the samples were characterized by XRD and EDS, and their optical features were measured by the 325 nm line of a He–Cd laser at room temperature. The electrical properties of the films were also investigated.

### 3. Results and discussions

The Cd<sub>1−*x*−*y*</sub>Fe<sub>*x*</sub>Zn<sub>*y*</sub>S films with low Fe content are yellow, very transparent with a very smooth surface. XRD data showed that the films are well crystallized. All of the films have a *c*-axis-preferred orientation and no peaks of other phases were detected, just as shown in Fig. 1. It can be seen that with increasing of the content of Fe and Zn, the peaks of the (0002) diffraction shift to larger angles. The reason for this is that both the radius of the Zn<sup>2+</sup> and the Fe<sup>2+</sup> are smaller than that of Cd<sup>2+</sup>. Meanwhile, the full width at half maximum (FWHM) of the XRD peaks becomes broader with the increase of the Fe and Zn dopants which is mostly due to the alloy fluctuation in samples. From Fig. 1, it can be concluded that highly preferred films could be prepared by LP-MOCVD even with high doping concentration. The compositions of Cd<sub>1−*x*−*y*</sub>Fe<sub>*x*</sub>Zn<sub>*y*</sub>S films were determined by EDS. The Fe concentration in Cd<sub>1−*x*−*y*</sub>Fe<sub>*x*</sub>Zn<sub>*y*</sub>S films ranges from 0 to 0.35 (0 < *x* < 0.35), while that is 0 to 0.4 in Cd<sub>1−*x*</sub>Fe<sub>*x*</sub>S films (0 < *x* < 0.4). It was indicated that Zn-doping could reduce the Fe-doping concentration slightly due to that Zn atom is easier to react with S than Fe atom. Therefore, the competition between Zn and Fe reacting with S caused the reduction of the Fe-doping concentration. The energy

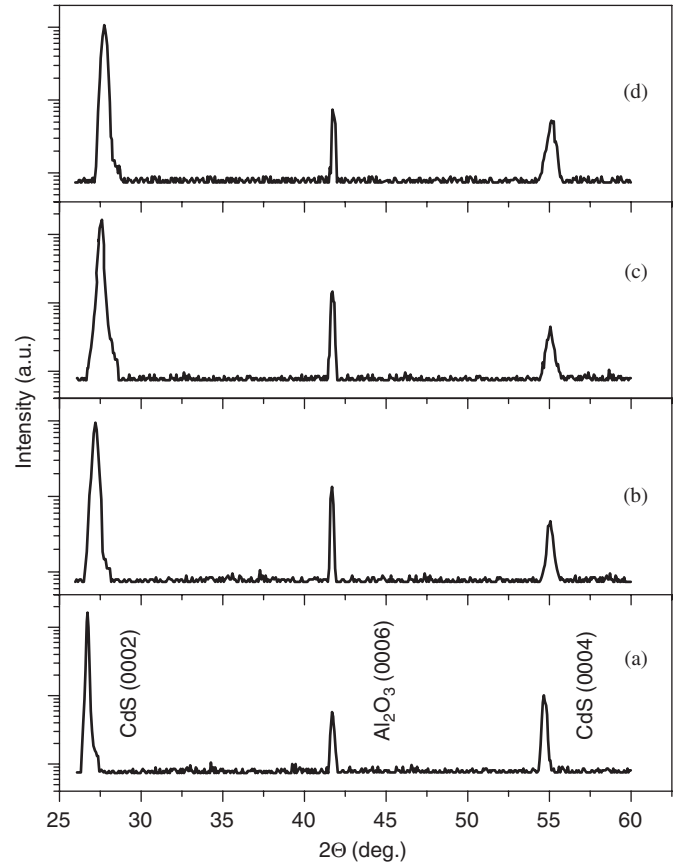


Fig. 1. XRD patterns of CdS (a), Cd<sub>0.88</sub>Fe<sub>0.08</sub>Zn<sub>0.04</sub>S (b), Cd<sub>0.8</sub>Fe<sub>0.09</sub>Zn<sub>0.11</sub>S and (c), Cd<sub>0.61</sub>Fe<sub>0.32</sub>Zn<sub>0.07</sub>S (d).

gap of Cd<sub>1−*x*−*y*</sub>Fe<sub>*x*</sub>Zn<sub>*y*</sub>S films can be obtained from the optical absorption spectra, just as shown in Fig. 2(a). The determination of the fundamental absorption gap and the fitting processing are performed as reported by David Dutton [20]. The sharp absorption edges of samples *a*, *b* and *c* confirms the good optical property of the Cd<sub>1−*x*−*y*</sub>Fe<sub>*x*</sub>Zn<sub>*y*</sub>S films. However, with further increase of the Fe composition, the slopes of the absorption edges become gentler. According to the optical absorption spectra of Fe-doped CdS in Fig. 2(b), it can be concluded that the slopes of the absorption edges become gentler with increasing Fe content, which possibly originates from the alloy fluctuation, defects absorption, Fe<sup>2+</sup> intra-ion absorption and large exchange interaction of electrons in conduction and valence bands with the d electrons of Fe. Meanwhile, with the increase of Fe content, the absorption edges of CdFeS films shift to lower energy side due to the narrow band gap of FeS. Furthermore, comparing

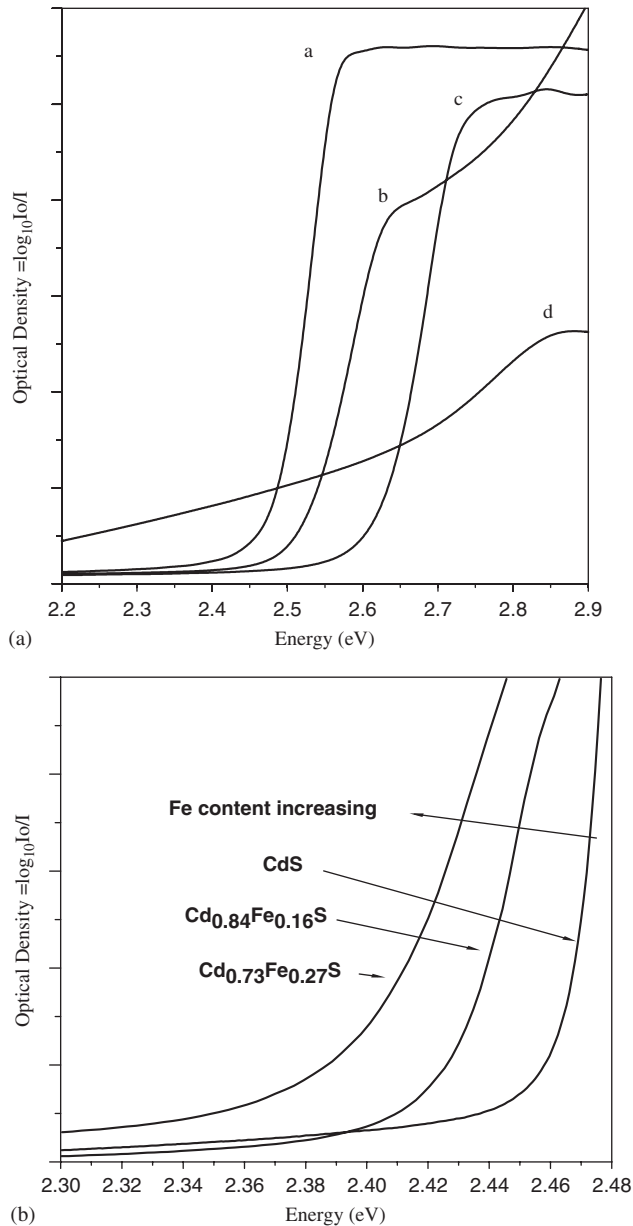


Fig. 2. (a) Band gap determination of the films with different compositions: (a)  $\text{Cd}_{0.88}\text{Fe}_{0.08}\text{Zn}_{0.04}\text{S}$ , (b)  $\text{Cd}_{0.84}\text{Fe}_{0.1}\text{Zn}_{0.06}\text{S}$ , (c)  $\text{Cd}_{0.8}\text{Fe}_{0.09}\text{Zn}_{0.11}\text{S}$ , and (d)  $\text{Cd}_{0.60}\text{Fe}_{0.35}\text{Zn}_{0.05}\text{S}$ . (b) Band gap determination of the  $\text{CdS}$ ,  $\text{Cd}_{0.84}\text{Fe}_{0.16}\text{S}$  and  $\text{Cd}_{0.73}\text{Fe}_{0.27}\text{S}$ . The thickness of the films is 800 nm.

Fig. 2(a) with (b), it can be observed that Zn-doping could lead to remarkable increase of the band gap because the band gap of ZnS is much wider than that of CdS. Therefore, we could adjust the band gap energy in a wide range by changing the Zn composition. In order to study the effect of impurity on the optical properties, the photoluminescence (PL) spectra of the  $\text{Cd}_{0.8}\text{Fe}_{0.09}\text{Zn}_{0.11}\text{S}$ ,  $\text{Cd}_{0.91}\text{Fe}_{0.09}\text{S}$  and CdS films at room temperature are investigated as shown in Fig. 3. The PL peak position of  $\text{Cd}_{0.91}\text{Fe}_{0.09}\text{S}$  shifts to the lower energies side compared with that of CdS. The reason for this trend is that the band gap of FeS is narrower than that of CdS. When doped with

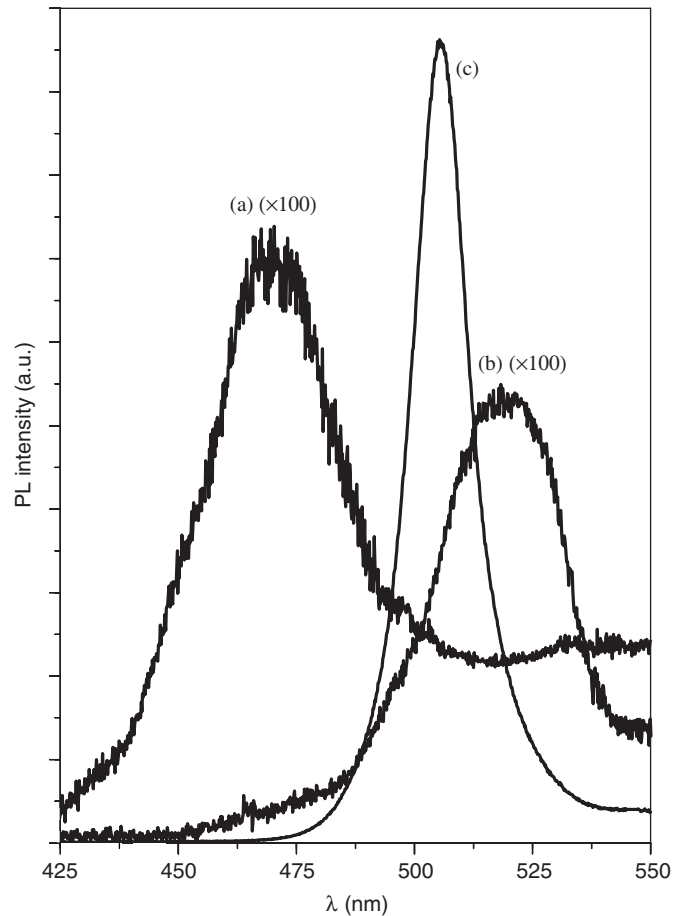


Fig. 3. PL spectra of: (a)  $\text{Cd}_{0.8}\text{Fe}_{0.09}\text{Zn}_{0.11}\text{S}$ , (b)  $\text{Cd}_{0.91}\text{Fe}_{0.09}\text{S}$  and (c) CdS at room temperature.

Zn atoms, the PL peak position of  $\text{Cd}_{0.8}\text{Fe}_{0.09}\text{Zn}_{0.11}\text{S}$  shifts to the higher energies due to the band gap of ZnS is much wider than that of CdS and the content of Zn is larger than Fe. This result is good agreement with the optical absorption spectra shown in Fig. 2. The FWHM of the peak becomes broader with the increase of dopant content, which can be explained by the alloy fluctuations and the defects in the films. The PL peaks are attributed to the band-edge emission.

The electrical properties of the films are also measured, as summarized in Table 2. All the films showed a resistivity of  $10^4$ – $10^3 \Omega\text{cm}$  and did not have big change with changing the dopant concentration when a magnetic field of 15000 Oe was applied. This result is much different from that of (Mn, Co) co-doped ZnO thin films reported by Yan et al. [19] and Gu et al. [21]. However, we find that the carrier density changes three orders of magnitude for the samples with different Fe and Zn doping concentration. Since the ions of Zn and Fe substituting for Cd in CdFeZnS films are isoelectronic centers and could not act as donor or acceptor, the change in carrier density from  $10^{12}$  to  $10^{15} \text{cm}^{-3}$  might relate to the intrinsic defects or unintentionally incorporated impurities in the CdFeZnS films. In addition,  $\text{Cd}_{0.60}\text{Fe}_{0.35}\text{Zn}_{0.05}\text{S}$  film which is with the

Table 2  
Resistivity, Hall coefficient, carrier density and Hall mobility of the films

Film	Resistivity ( $\Omega\text{cm}$ )	Hall coefficient ( $\text{cm}^3/\text{C}$ )	Carrier density ( $\text{cm}^{-3}$ )	Hall mobility ( $\text{cm}^2/\text{Vs}$ )	Type
$\text{Cd}_{0.88}\text{Fe}_{0.12}\text{S}$	$6.7519 \times 10^3$	$3.8525 \times 10^4$	$1.6203 \times 10^{14}$	6.2028	p
$\text{Cd}_{0.84}\text{Fe}_{0.16}\text{S}$	$1.3226 \times 10^5$	$9.6386 \times 10^5$	$6.4762 \times 10^{12}$	7.6446	p
$\text{Cd}_{0.60}\text{Fe}_{0.35}\text{Zn}_{0.05}\text{S}$	$4.5422 \times 10^4$	$3.0721 \times 10^4$	$1.4019 \times 10^{15}$	0.0918	p
$\text{Cd}_{0.88}\text{Fe}_{0.08}\text{Zn}_{0.04}\text{S}$	$5.8388 \times 10^4$	$5.6467 \times 10^4$	$1.1055 \times 10^{14}$	6.2324	P
$\text{Cd}_{0.8}\text{Fe}_{0.09}\text{Zn}_{0.11}\text{S}$	$2.4287 \times 10^4$	$-1.4142 \times 10^5$	$4.4141 \times 10^{13}$	6.2504	n
$\text{Cd}_{0.84}\text{Fe}_{0.1}\text{Zn}_{0.06}\text{S}$	$2.9009 \times 10^4$	$-1.0172 \times 10^5$	$6.1369 \times 10^{13}$	3.5823	n

highest Fe concentration has the lowest Hall mobility. This indicates that the quality of the films was deteriorated with increasing Fe dopant concentration to a large amount.

#### 4. Conclusions

High-quality  $\text{Cd}_{1-x}\text{Fe}_x\text{S}$  and  $\text{Cd}_{1-x-y}\text{Fe}_x\text{Zn}_y\text{S}$  thin films were grown on  $c\text{-Al}_2\text{O}_3$  substrates by LP-MOCVD at  $360^\circ\text{C}$  and with the pressure of 76 Torr. The films have only (0002) diffraction peaks in XRD pattern. Due to the doping of Zn, we could not only adjust the band gap energy in wide range, but also could control the doping content of Fe.  $\text{Cd}_{1-x-y}\text{Fe}_x\text{Zn}_y\text{S}$  thin films had good crystal quality with the Fe content below 0.3. According to this result,  $\text{CdFeZnS}$  films could be a promising material for applications of magneto-optical devices and solar cells.

#### Acknowledgments

This work is supported by the National Natural Science Foundation of China under Grant no. 50402016 and no. 60278031; the Key Project of National Natural Science Foundation of China under Grant no. 60336020, the Innovation Project of Chinese Academy of Sciences.

#### References

- [1] J.K. Furdyna, J. Appl. Phys. 64 (1988) R29.
- [2] S.A. Wolff, et al., Science 294 (2001) 1488.
- [3] Y.H. Hwang, Y.H. Um, J.K. Furdyna, Semicond. Sci. Technol. 19 (2004) 565.
- [4] H. Ohno, Science 281 (1998) 951; H. Ohno, J. Magn. Mater. 200 (1999) 110.
- [5] H. Munekata, H. Ohno, S. von Molnar, A. Segmuller, L.L. Chang, L. Esaki, Phys. Rev. Lett. 63 (1989) 1849.
- [6] H. Ohno, A. Shen, F. Matsukura, A. Oiwa, A. Endo, Y. Iye, Appl. Phys. Lett. 69 (1996) 363.
- [7] A. Twardowski, T. Dietl, M. Demianiuk, Solid State Commun. 48 (1983) 845.
- [8] A. Twardowski, M.V. Ortenberg, M. Demianiuk, R. Pauthenet, Solid State Commun. 51 (1984) 849.
- [9] J.K. Furdyna, N. Samarth, J. Appl. Phys. 61 (1987) 3526.
- [10] T. Mina, S. Satyam, K.J. Prafulla, Phys. B: Condens. Matter 348 (2004) 235.
- [11] T. Miura, Y. Yamamoto, S. Itaya, K. Suga, K. Kindo, T. Takenobu, Y. Iwasa, H. Hori, Phys. B: Condens. Matter 346–347 (2004) 402.
- [12] V. Zayets, M.C. Debnath, K. Ando, Appl. Phys. Lett. 84 (2004) 565.
- [13] R. Rey-de-Castro, D. Wang, X. Zheng, A. Verevkin, R. Sobolewski, M. Mikulic, R. Adam, P. Kordos, A. Mycielski, Appl. Phys. Lett. 85 (2004) 3806.
- [14] B.Y. Geng, L.D. Zhang, G.Z. Wang, T. Xie, Y.G. Zhang, G.W. Meng, Appl. Phys. Lett. 84 (2004) 2157.
- [15] Y.Q. Chang, D.B. Wang, X.H. Luo, X.Y. Luo, X.Y. Xu, X.H. Chen, L. Li, C.P. Chen, R.M. Wang, J. Xu, D.P. Yu, Appl. Phys. Lett. 83 (2003) 4020.
- [16] M. Imamura, J.Y. Ahn, A. Okada, K. Takashima, J. Appl. Phys. 95 (2004) 6876.
- [17] S.-J. Han, J.W. Song, C.-H. Yang, S.H. Park, J.-H. Park, Y.H. Jeong, K.W. Rhie, Appl. Phys. Lett. 81 (2002) 4212.
- [18] N.H. Hong, V. Brize, J. Sakai, Appl. Phys. Lett. 86 (2005) 082505.
- [19] L. Yan, C.K. Ong, X.S. Rao, J. Appl. Phys. 96 (2004) 508.
- [20] D. David, Phys. Rev. 112 (1958) 785.
- [21] Z.-B. Gu, C.-S. Yuan, M.-H. Lu, J. Wang, D. Wu, S.-T. Zhang, S.-N. Zhu, Y.-Y. Zhu, Y.-F. Chen, J. Appl. Phys. 98 (2005) 053908.